Bull. Soc. géol. France, 1996, n. s., n° 170, pp. 43-52

III

Wide-angle reflection seismics in the western Alps

F. THOUVENOT, A. PAUL, G. SENECHAL, A. HIRN, R. NICOLICH
and the ECORS-CROP Deep Seismic Sounding Group

III.A. – Introduction

Because of their heterogeneity, the Alps can be considered a real challenge when modelling the bowels of the Earth. Even if we aim – as we do here – to the topography of only a few major deep interfaces, the problem can in no way be tackled as it is elsewhere in more quiet tectonic settings. The Moho discontinuity, unquestionably the major interface in the continental lithosphere, bears evidence, through its position and topography, of the regional geodynamics. As such, any reconnaissance survey of the deep structures should bring it into focus.

As Moho data were collected in the western Alps in the last decades, successive Moho maps [Closs and Labrouste, 1963; Labrouste *et al.*, 1968; Choudhury *et al.*, 1971; Perrier, 1973; Giese and Prodehl, 1976] soon revealed the dip to the east of the Moho beneath the Alpine foreland. An anomalously shallow structure (the Ivrea body) was also detected, that covered the deep autochthonous Moho in the inner zones.

To account for the complexity of the Alps, it was first thought that the easiest layout to collect Moho data in the belt was to design strike profiles – e.g. ALP75 experiment from France to Hungary [Alpine Explosion Seismology Group, 1976] –: with the structures being sampled longitudinally, the interpretation hopefully keeps one-dimensional. Another way to proceed – e.g. profiles connected to the European Geotraverse (EGT) experiment in 1983 [Thouvenot *et al.*, 1985] – is to traverse the belt perpendicularly to the strike. Of course, one can expect the record-sections to be more complex because a two-dimensional modelling now has to be dealt with. However, this kind of profiling is suitable for observing late arrivals – reflections from a deep Moho – as well as anomalous first arrivals, for instance produced by waves travelling through the Ivrea body.

III.B. – The 1985 experiment

The Moho information provided by these layouts is obviously limited : even if transverse profiles allow a simultaneous investigation of different tectonic regions, the Moho topography made available is restricted to a zone a few tens of kilometres long at best. This is mainly due to the heterogeneity of the Alpine crust that allows reflections from the Moho to be observed only around the so-called **critical distance** (in the 90-140 km range, depending on the depth of the reflector).

When it was decided in 1985 to complement the planned ECORS-CROP vertical reflection line (VRL) with a deep seismic sounding survey, it was considered that the best way to get a clear Moho picture across the western Alps was to use 5 shot-points (fig. III-1), and record them to the north and south along several fans, with an observation distance chosen close to the critical distance. Every station on the fan is most suitably placed to record a very high amplitude seismic signal that corresponds to total reflection from the Moho. The angle of incidence of the seismic ray on the reflector is large (around 50°) – hence the name of wide-angle reflection (WAR) that will be henceforth applied to this technique.

This method had already proved successful in other orogenic belts [e.g. Hirn *et al.*, 1980 and 1987]. Aimed at mapping only deep interfaces and carried out one year prior to the VRL, our reconnaissance survey can in no way compete with the roadroller strength of the vertical seismics, that provide a more complete crustal image. Using more versatile equipments, illuminating deep reflectors with different frequencies and angles of incidence, the method is however bound to bring important constraints on the physical properties of the deep crust.

III.C. – The northern fans

We will first address data obtained along the northern fans (fig. III-1). About 30 stations were deployed every 4 km on each fan. For each shot-station couple, the reflection point is plotted half-way, so that each fan provides by itself a cross-section with the reflectors being sampled every 2 km. Because of logistics, these cross-sections have overlaps or offsets, so that it seems difficult to speak in terms of a single cross-section of the belt. The composite cross-section presented in figure III-2 shows in its upper part the combination of fans A, B and C (western fans) and in its lower part the combination of fans D and LW (eastern fans).

The cross-section in figure III-2a extends from the Subalpine ranges through the Belledonne External Crystalline Massif (ECM), to the Dora Maira Internal Crystalline Massif (ICM). Each seismic trace was processed so that the time scale is converted to depth using a mean crustal velocity, here chosen as 6.25 km/s^{-1} [ECORS-CROP Deep Seismic Sounding Group, 1989]. The maximum energy of the signal corresponds to the Moho reflection. Almost flat at about 37 km beneath the Subalpine ranges, the Moho then dips to the east to reach a maximum depth of about 55 km beneath the French-Italian border. This dip is observed using data from shots A and B. Results for shot C were quite unexpected : they show a relatively shallow reflective zone between 23 and 29 km that was not reached by shot B. This is a clue to the limited extent of this reflector : when shooting from B, we reach the deep Moho; when shooting from C, this reflector acts as a mask that prevents the seismic energy wawes from penetrating deeper in the crust.

The second cross-section (fig. III-2b) is closer to the VRL and extends from the Gran Paradiso ICM through the Sesia Massif to the Po Plain. A reflector beneath the Sesia Massif can be evidenced at 13 km, more or less in coincidence with the Ivrea body. But what is especially clear here is how the Po Plain Moho deepens from 25 to 35 km. The phase correlation presented here involves a stepwise dee-

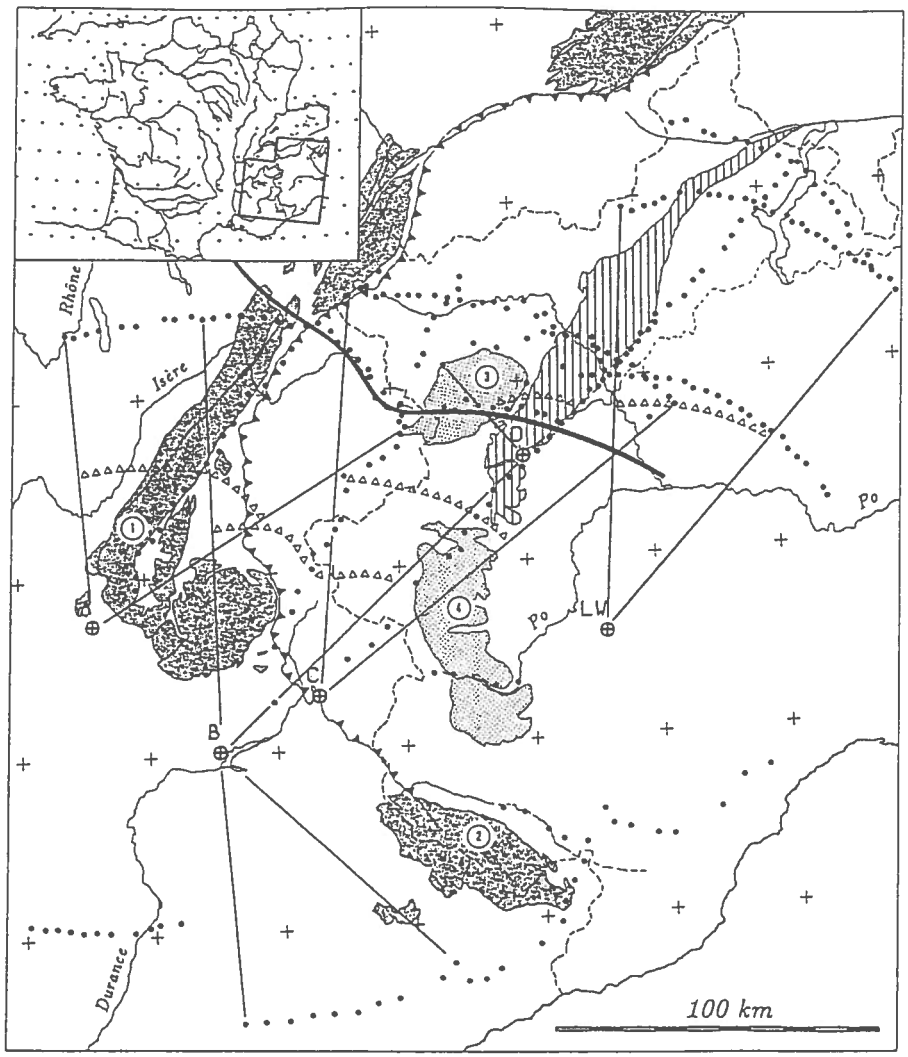

FIG. III-1. – Complete position map of the layout. Shot-points were recorded by stations (full circles) deployed along longitudinal profiles and fans [after Thouvenot *et al.*, 1990]. Open triangles indicate reflection points for the 5 fans used to build up figure 2. Shaded area = External Crystalline Massifs (1 = Belledonne; 2 = Argentera); dotted area = Internal Crystalline Massifs (3 = Gran Paradiso; 4 = Dora Maira); hatched area = Sesia-Lanzo unit. Penninic frontal thrust identified by solid triangles. Heavy line marks ECORS-CROP vertical reflection line (VRL).

FIG. III-1. – *Positionnement du dispositif. Les tirs ont été enregistrés par des stations (cercles pleins) déployées le long de profils longitudinaux ou en éventails [d'après Thouvenot* et al., *1990]. Les triangles évidés indiquent les points de réflexion pour les 5 éventails utilisés pour construire la figure 2. Zones grisées : Massifs Cristallins Externes (1 = Belledonne ; 2 = Argentera) ; pointillés = Massifs Cristallins Internes (3 = Grand Paradis ; 4 = Dora Maira) ; hachures : unité de Sesia-Lanzo. Le chevauchement pennique frontal est souligné par des triangles. Les traits épais correspondent aux profils ECORS-CROP.*

pening. Of course this way of seeing can be argued against, because we reach here the resolution limit of the sampling.

However, fan profiles subsequently recorded in northern Italy as part of the EGT'86 experiment seem to support this idea. One of these fan profiles recorded a shot-point much farther to the east (fig. III-3a), which provides a north-south cross-section of the Po Plain (fig. III-3b). (This cross-section happens to complement ours at right angle; see fig. III-1). Results obtained by Nadir [1988] show a Moho undoubtly deepening by steep faults between 30 and 45 km. The depth of 35 km obtained at about the third of the section is consistent with the depth reached in the eastern end of our section (fig. III-2b), where the two profiles meet. To the south, the Moho topography shown by figure III-3b is more complex due to the imbrication of the Ligurian Moho.

III.D. – COMPARISON WITH THE VERTICAL REFLECTION LINE

The shallow reflector which are overthrusting the deep Moho in the Penninic zone, had never been mapped before, hence our marked interest in it. The reflection points that sample this reflector are located beneath the Ambin Massif and the Upper Dora Riparia Valley, more than 30 km off the VRL. For the deep Moho reached when shooting from B, the mirror points are in the Montgenèvre area, 60 km south of the VRL (figs. III-1 and -4).

There is therefore an unavoidable problem of projection if one wants to take these reflectors into account when interpreting the VRL data, and there are of course different ways to proceed. For instance, projections perpendicular to the mean trend of the VRL can be used (fig. III-4a) – but

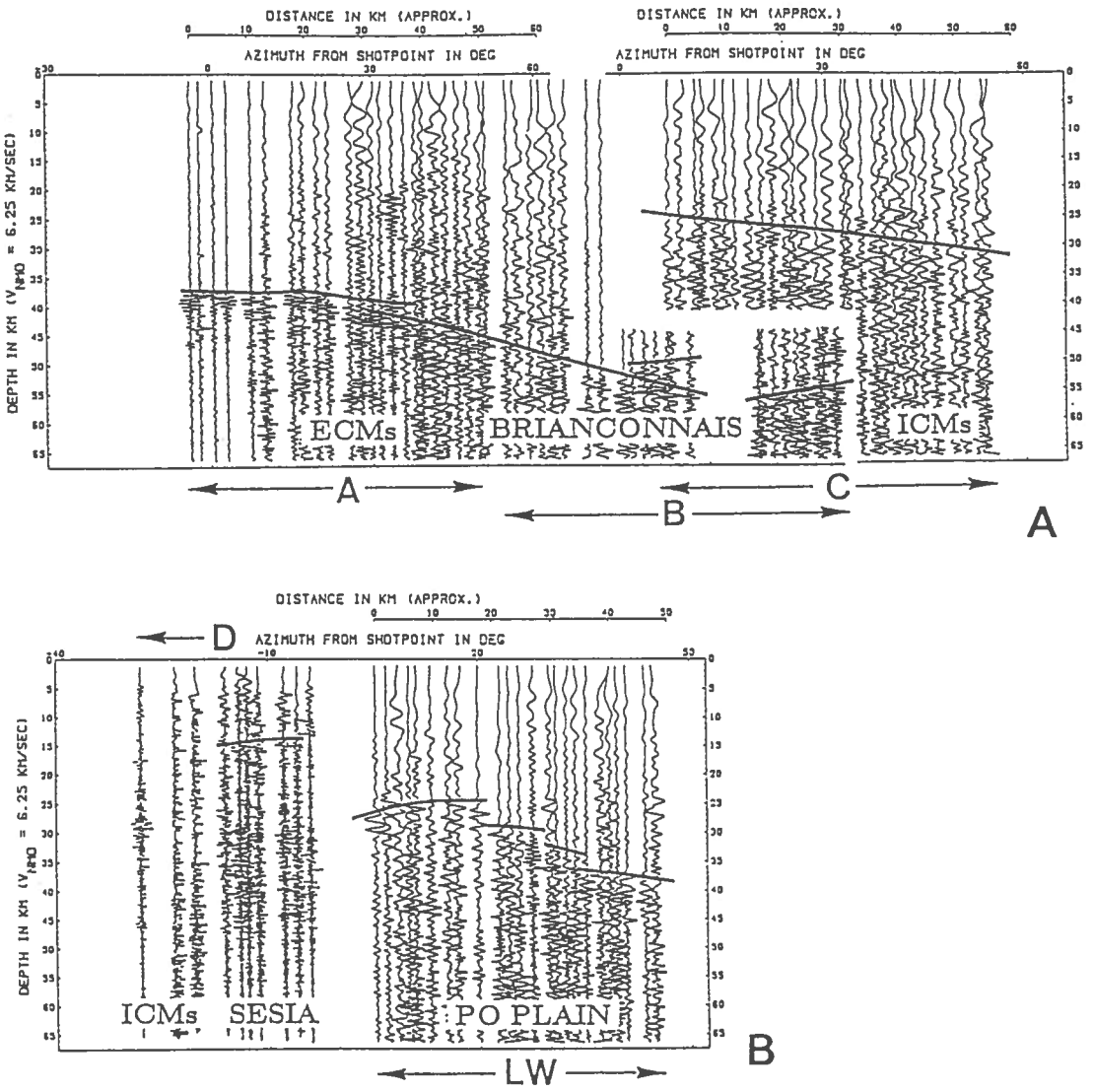

FIG. III-2. – Two pseudo cross-sections of the western Alps : (A) the three northern fan profiles from shot-points A, B and C (see position in fig. 1) are combined as a single record-section extending from the Subalpine ranges (far left) to the Dora Maira massif (far right); (B) this shorter section combines results from shot-points D and LW and extends from the Gran Paradiso massif (far left) to the Po Plain (far right) [after Thouvenot *et al.*, 1990].

FIG. III-2. – *Deux coupes synthétiques à travers les Alpes occidentales :* (A) *les trois éventails septentrionaux correspondants aux points de tir* A, B *et* C *(voir position sur fig. 1), ont été combinés sur un seul enregistrement allant des massifs sub-alpins (extrême gauche) jusqu'au massif de Dora Maira (extrême droite);* (B) *cette coupe plus courte combine les résultats des tirs* D *et* LW *et va du massif du Grand Paradis (extrême gauche) jusqu'à la Plaine du Pô (extrême droite) [d'après Thouvenot* et al., *1990].*

which trend should we consider, given the VRL is crooked. It might be eventually more sensible to use the local Bouguer isolines as guide lines for the projection (fig. III-4b), because they reflect the way deep structures continue.

Depending on the choice, the results will differ by some tens of kilometres. The westernmost part of the shallow reflector will be projected between Séez and Val d'Isère, with its easternmost end around Pont Canavese. The deep autochthonous Moho should be located in the VRL between Séez and La Galise Pass, or between La Galise Pass and Noasca. This horizontal uncertainty is increased by a vertical uncertainty (although the latter is likely to be lessened if the projection used the local Bouguer isolines, which should prevent any dip effect of the deep structures). In conclusion, even if it is tempting to directly plot the wide-angle reflectors onto the vertical reflection line-drawing, we should keep a critical eye on it, and remember that this superposition is not well constrained, neither horizontally nor vertically.

Instead of blindly merging the two types of data, we found it more advisable to separate in figure III-5 the results of the two methods (vertical reflection seismics in fig. III-5a; wide-angle seismics in fig. III-5b). The NW-SE cross-section extends from the Penninic frontal thrust to the Po Plain, and both data sets have been processed to migrate the reflectors into their actual positions. To this purpose, the line-drawings – either vertical reflection or wide-angle – were first digitized. Allowance was made for the quality of the reflections (heavy or thin lines), strict elevation corrections were computed for the wide-angle data. Velocity was eventually allowed to vary throughout the model, both vertically and horizontally. The depth scale is referred to the sea level.

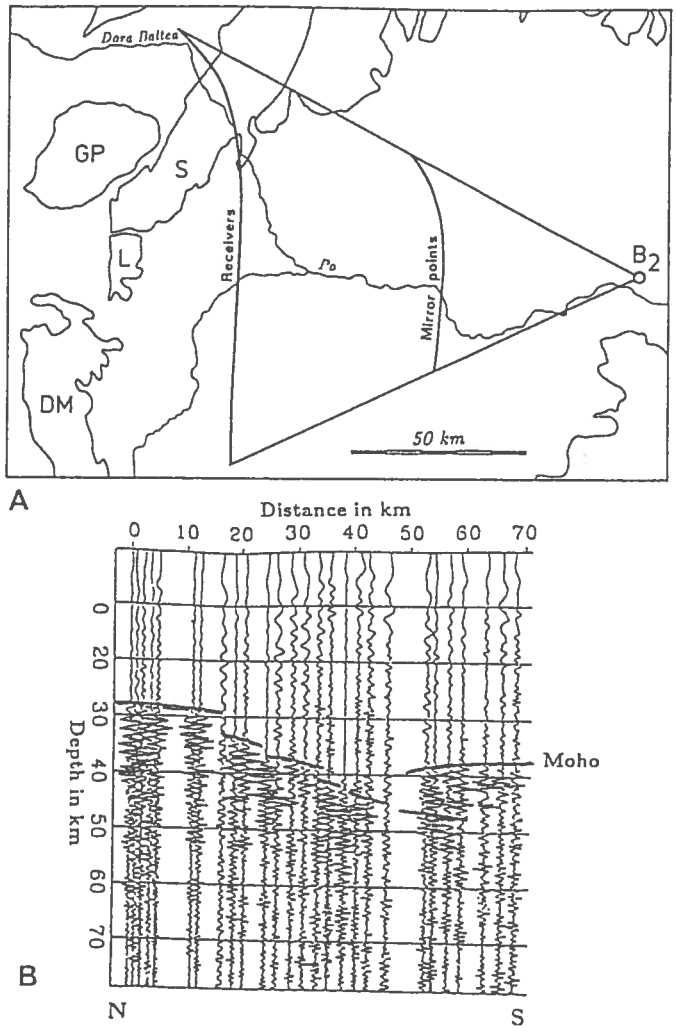

FIG. III-3. – An example of fan profile in the Po Plain (EGT'86 experiment) : (A) Schematic position map with shot-point B_2, the recording array and the corresponding mirror points. DM = Dora Maira ; GP = Gran Paradiso ; L = Lanzo unit ; S = Sesia unit ; (B) North-south cross-section of the western Po Plain [Nadir, 1988] showing the septwise deepening of the Moho. Compare with figure 2 B.

FIG. III-3. – *Exemple de profil en éventail sous la Plaine du Pô (campagne EGT 86) :* (A) *positionement schématique du point B2, le système d'enregistrement et les points miroir correspondants.* DM = *Dora Maira ;* GP = *Grand Paradis ;* L = *unité de Lanzo ;* S = *unité de Sesia ;* (B) *coupe nord-sud à travers la Plaine du Pô [Nadir, 1988], montrant l'approfondissement par paliers du Moho. Comparer avec la figure III-2 B.*

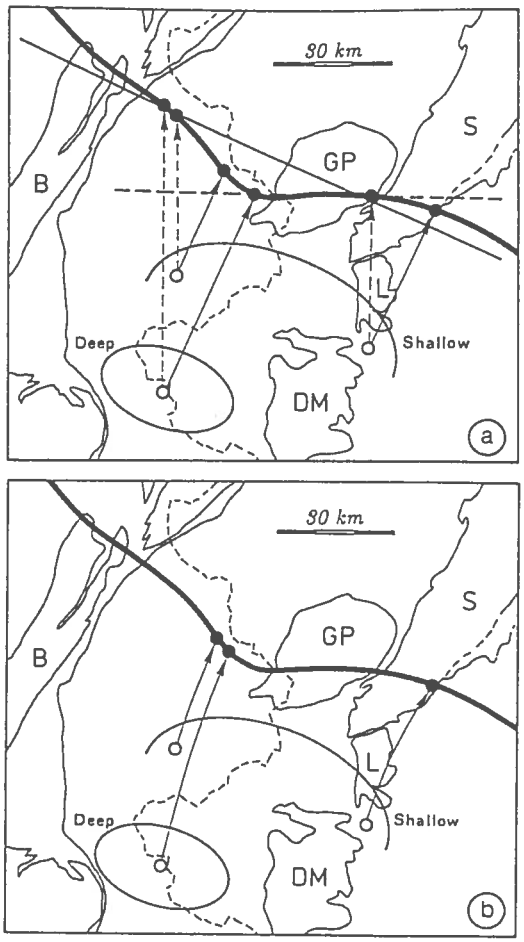

FIG. III-4. – Different ways to project the wide-angle data – deep autochthonous Moho and shallow reflective unit – onto the VRL (heavy line) [after Thouvenot *et al.*, 1990]. (a) Orthogonal projection on the mean trend of the VRL showing an allowance due to the crooked line. (b) Projection along the local Bouguer isolines. B = Belledonne ; DM = Dora Maira ; GP = Gran Paradiso ; L = Lanzo unit ; S = Sesia unit.

FIG. III-4. – *Différentes méthodes de projection des données grand-angle – Moho autochtone et réflecteurs peu profonds – sur le profil de réflexion profonde (trait épais) [d'après Thouvenot* et al., *1990].* (a) *Projection orthogonale à la direction moyenne du profil de sismique réflexion, en lissant ses sinuosités.* (b) *Projection parallèle aux courbes d'iso-valeurs de l'anomalie de Bouguer.* B = *Belledonne ;* DM = *Dora Maira ;* GP = *Grand Paradis ;* L = *unité de Lanzo ;* S = *unité de Sesia.*

The main result in figure III-5a is the apparent transparency of the crust below 20-25 km, while the upper crust is very reflective [Bayer *et al.*, 1987 ; Tardy *et al.*, 1990]. This depth range where the reflectivity disappears is precisely where we find, in figure III-5b, the shallow wide-angle reflector. Figure III-5b can however be misleading, because it suggests that this shallow reflector terminates in the middle of the section. Let alone the projection problem discussed above, we have no actual constraint on the western limit of the reflector, simply because our fan layout for shot C did not extend that far west (fig. III-1). As for the deep autochthonous Moho, it could be detected by the wide-angle reflection seismics only.

This Moho picture along the two sections of figure III-2 is complemented, for the upper 20 kilometres of the crust, by in-line data, decisive in this depth range since most of the fans were designed to observe much deeper reflectors. From the three western shot-points, reflections recorded between 40 and 70 km in distance indicate interface situated in the 15-20 km depth range, at the base of the upper crust (fig. III-6). However, with data sampling units as different as the ECMs, the Briançonnais zone and the ICMs, these interfaces may not have all the same signification : although in the same depth interval, it does not seem sensible to correlate them to define a horizontally-layered intermediate crust across the Alpine arc. Surprisingly, the VRL data does not single out this depth interval as particularly reflective and continuous. As these shallow reflectors are detected close to the shot-points – more than 50 km south of the vertical reflection line –, this could be the effect of a structural variation along the strike of the Alps.

Shot-point D, situated in the Lanzo ultramafic massif, was also recorded in-line along a profile stretching northwards through the Sesia unit (fig. III-1). The apparent velocity of first arrivals observed at short distance are significantly higher than in the western units. In a flat-layered model, this would indicate the presence of rocks of

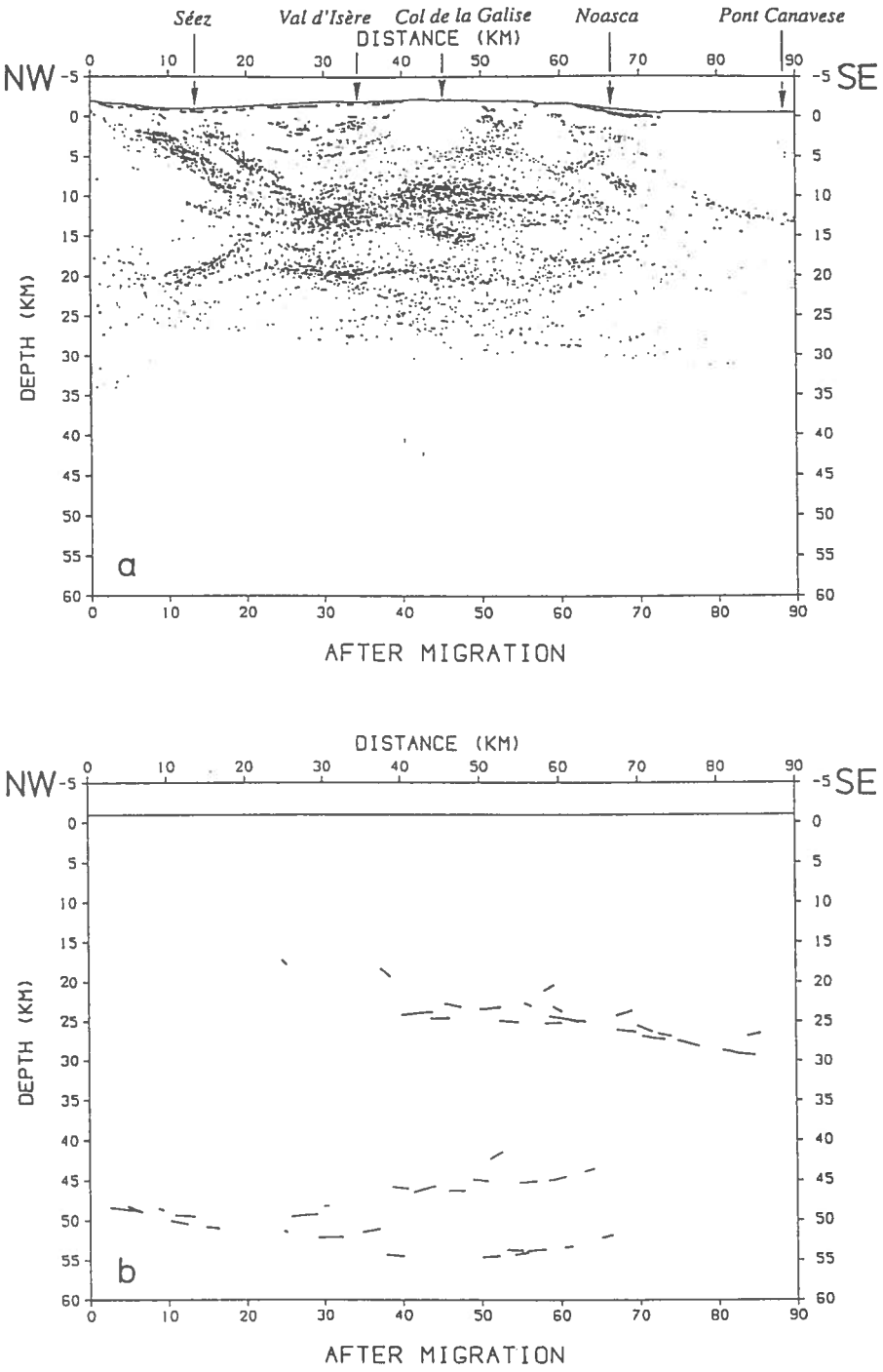

G. III-5. – Two NW-SE cross-sections, from the Penninic frontal thrust to the Po Plain, showing the seismic reflections after migration :
(a) VRL data. In the central part of the section, note the high reflectivity in the 10-15 km depth range and a deeper reflective level at a depth of out 20 km. Very few reflections can be detected below it ;
(b) Wide-angle data. The autochthonous Moho – maximum depth of about 55 km – is overlain by a shallow reflective unit in the same depth range, ıere the VRL data show that reflectivity stops [after Thouvenot *et al.*, 1990].

G. III-5. – *Deux coupes NW-SE allant du front pennique à la Plaine du Pô et montrant les réflecteurs sismiques après migration :*
(a) données de sismique réflexion verticale. Dans la partie centrale de la section, on observe une zone à forte réflectivité entre 10 et 15 km, et un veau réflecteur plus profond à 20 km. Peu de réflexions peuvent être enregistrées à plus grande profondeur ;
(b) données grand-angle. Le Moho autochtone – profondeur maximale de 55 km – est surmonté par des réflecteurs qui n'ont pû être imagés sur la mique réflexion verticale [d'après Thouvenot et al., *1990].*

3 km.s^{-1} at only 5 km depth. Further velocity contrasts approximately 15 and 25 km depth are needed to account ır later reflections (the short-range fan profile from D ready detected a 13 km deep reflector in fig. III-2b). This the region near the top of the Ivrea gravimetric high, where mafic granulites and ultramafic rocks crop out and where former deep seismic experiments postulated the presence of lower crustal or anomalous upper mantle material only 5 to 10 km deep, with apparent velocities as high as 7.4 km.s^{-1}. But, as the present profiles are unreversed like

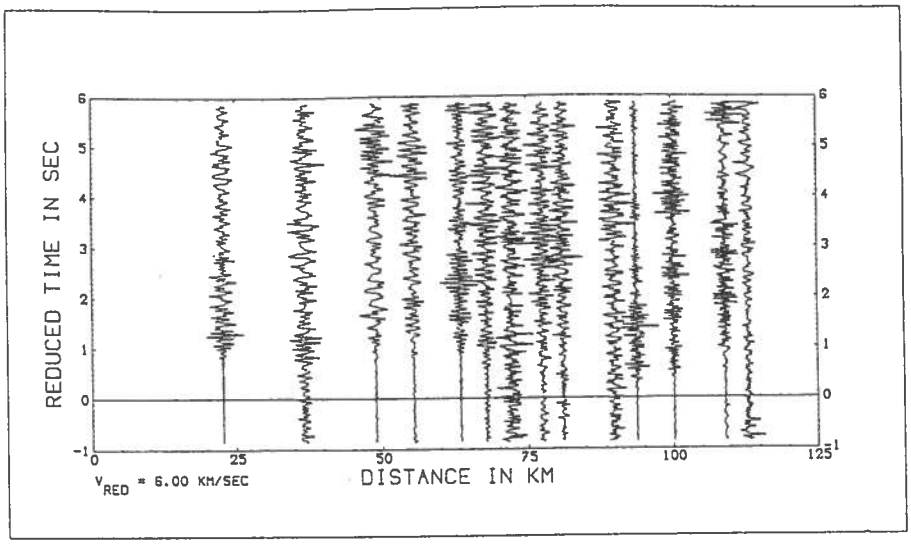

FIG. III-6. – A close-up of the longitudinal profile recording shot B towards the northeast. Intracrustal reflections can be observed in the 15-20 km depth range.

FIG. III-6. – *Détail de l'enregistrement longitudinal du tir B vers le nord-est. Des réflexions intracrustales sont imagées entre 15 et 20 km.*

all the previous ones, we have no better constraints on the exact velocities, depths and geometries of what appears definitely as a high-velocity body.

III.E. – SHEAR-WAVE IMAGERY

Shear-wave observations are rare in crustal structure experiments : these experiments are very often carried out with vertical-component sensors only, and S-wave generation by explosions is anyway generally ineffective. Here also, only stations on the fans were equiped with 3-component seismometers. Figure III-7 shows an example of the western fan (shot-point A) for S waves recorded on horizontal components. To convert the time into the depth domain, we used a mean S-velocity of 3.6 km.s^{-1}, which is in the usual $\sqrt{3}$ ratio to the 6.25 km.s^{-1} P-velocity.

The Moho reflection looks very similar to the corresponding P-wave picture of figure III-2a. But, amazingly, an intracrustal structure appears around 30 km at depth. In the eastern part of the S-section, the amplitude of this reflection is even larger than the one referred to the Moho 20 km deeper. This intracrustal reflector is here seen at wide angle with S-waves and not with P-waves, a situation at variance with those reported in Brittany [Hirn *et al.*, 1987] and the Black Forest [Holbrook *et al.*, 1987]. Strong P-reflections and the absence of S-reflections from within the crust in those regions could be accounted for by an only small increase – or even decrease – of the S-velocity with depth in the middle crust, in contrast to a significant increase of the P-velocity with depth. This interpretation is supported by the likely increase of the Poisson's ratio σ with depth when quartz-bearing upper crustal rocks (low σ) change to more intermediate lower crustal materials (higher σ).

Since the situation is reversed at 25 km depth under the central part of the section through the Alps, one might then in contrary think of a transition from intermediate mineralogy to upper crustal rocks with increasing depth. We would then have to appeal to a superposition of hinterland lower crust on top of foreland upper crust, which would achieve the observed crustal thickening. However, if such an interface could easily explain the absence of wide-angle P-reflections, the S-velocity would also decrease or only very slightly increase across it : anyway, the contrast would not be sufficient to generate the clear wide-angle reflections observed here.

An alternative suggestion for the situation in the Black Forest has been to imagine a cracked medium under low fluid saturation just above the interface to increase the P but not the S-velocity [Holbrook *et al.*, 1987]. The enhanced S-reflectivity seen here under the Alps would by analogy demand a layer of low S-velocity, fluid-saturated rock on top of the reflector. It might not be completely impossible if it has the meaning of the base of a thick thrust zone. Clearly, basically original information is provided by the S-wave record, but the interpretation is far from being unique in the present state of general knowledge.

III.F. – AZIMUTHAL EFFECTS

In addition to the northern fans, a few stations were laid out to the south of the shot-points along three shorter fans (fig. III-1). These fans do not join each other and we cannot speak here in terms of a continuous cross-section of the southern French Alps. However, this arrangement of stations allows qualitative comparisons with the data in the north.

Figure III-8 illustrates how shot B was recorded southwards, with reflection points beneath the Digne nappe (Haute-Provence Subalpine ranges). When comparing this section to the central part of the main northern section (fig. III-2a) – shot B observed northwards –, the Moho is found much shallower at approximately 38 km (*vs* 55 km to the north). Of course, this could be expected, since we sample here the Moho in a very external position in the arc. Actually, this value of 38 km should rather be brought into comparison with a similar depth of 37 km found for shot A northwards, with reflection points beneath the northern Subalpine ranges (fig. III-2a, left).

However, if we compare again figure III-8 to the central part of figure III-2a – same shot but different reflection mirrors –, a shift of the spectral content toward low fre-

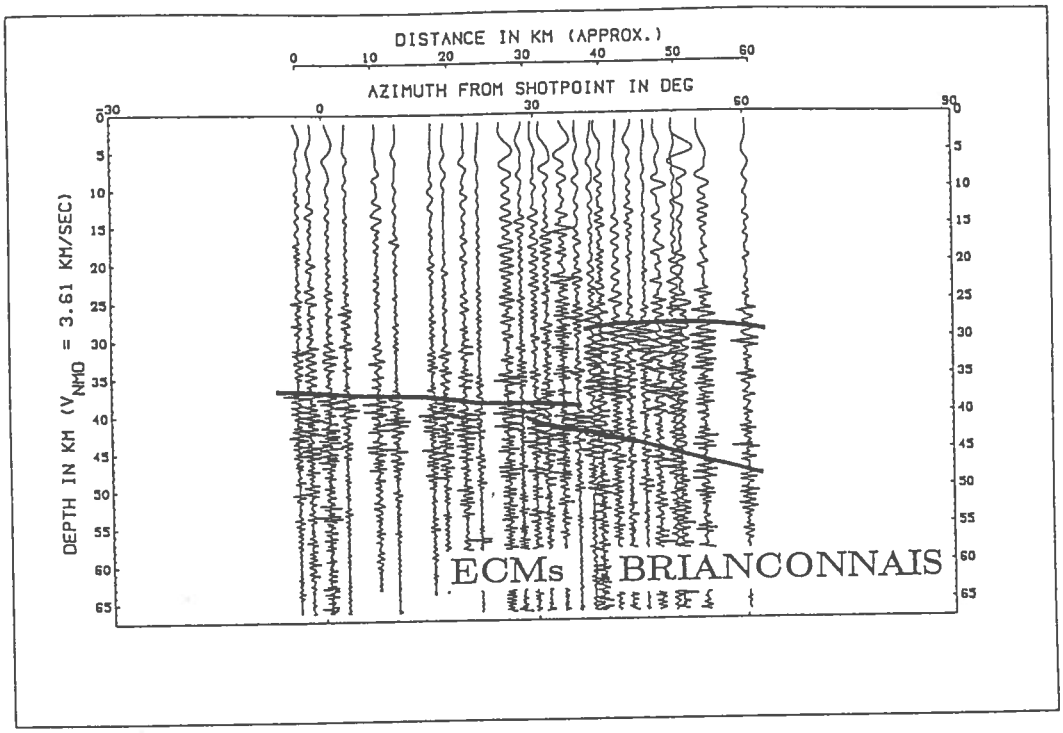

FIG. III-7. – The crust-mantle boundary in the external zone (far left on figure III-2a), as seen from S-wave data. If the Moho image is almost identical to the one given by P-waves, a mid-crustal reflective zone is enhanced beneath the Briançonnais. This zone was more or less transparent for P-waves on figure III-2a.

FIG. III-7. – *La limite croûte-manteau dans les zones externes (extrême gauche sur la figure III-2a), d'après les données ondes S. Bien que l'image du Moho soit pratiquement identique à celle donnée par les ondes P, des réflecteurs apparaissent dans la croûte moyenne sous le Briançonnais. Cette zone était quasiment transparente aux ondes P sur la figure III-2a.*

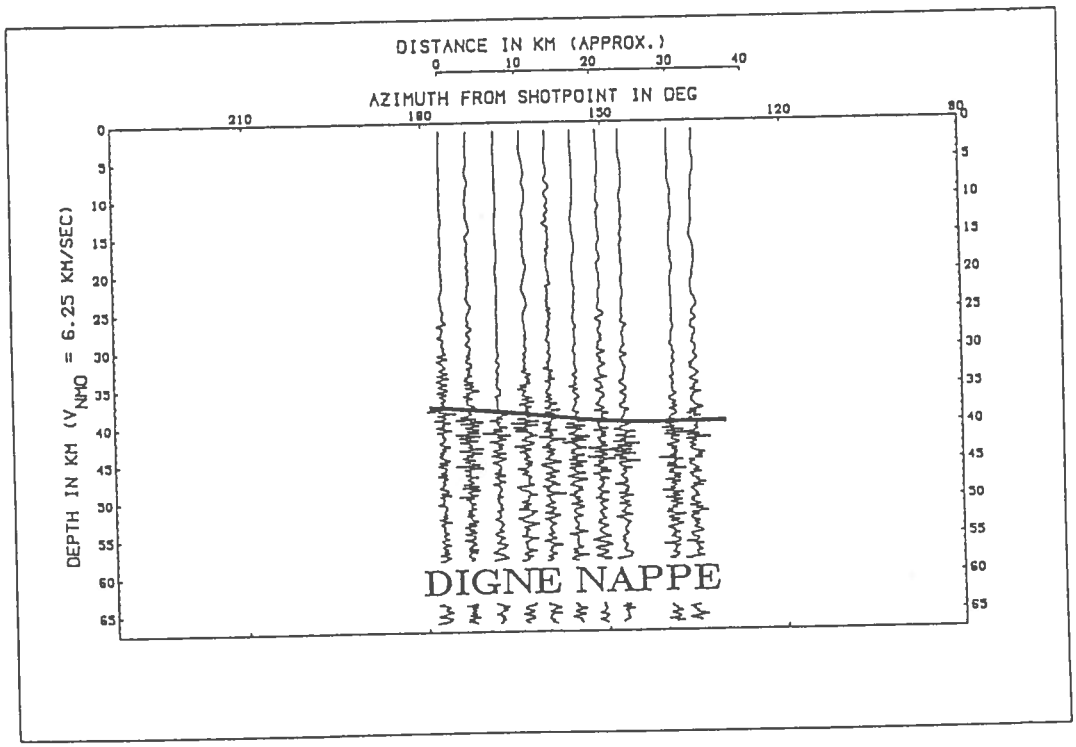

FIG. III-8. – Azimuthal dependence for wavelets reflected from the Moho. This W-E section across the Digne nappe (southern French Alps) records shot B southwards. Good quality reflections show a spectral content shifted towards high frequencies. Compare with the central part of section (a) on figure III-2, which shows shot-B recorded northwards.

FIG. III-8. – *Incidence de l'azimut sur les réflexions du Moho. Cette coupe E-W à travers la nappe de Digne (partie méridionale des Alpes françaises) a été batie à partir de l'écoute du point de tir B, situé plus au nord. Des réflexions de bonne qualité montrent un spectre déplacé vers les hautes fréquences. Comparer avec la partie centrale de la section* (a) *de la figure III-2, qui montre un enregistrement effectué au nord du point de tir B.*

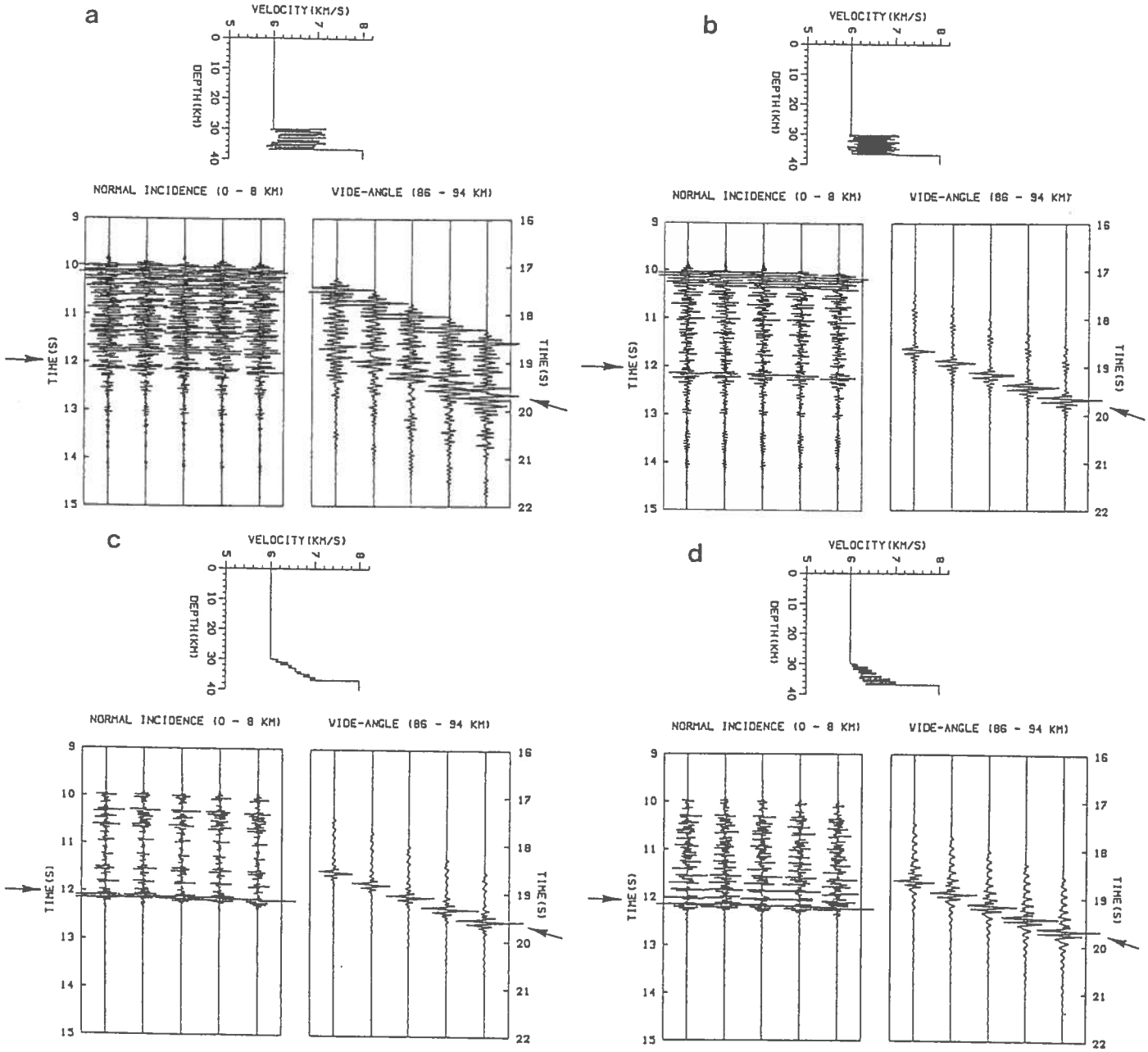

FIG. III-9. – Four examples of deep-crustal velocity models for the autochthonous Moho in the external zone (fig. III-2a, westernmost traces) and corresponding synthetic seismograms (left : normal incidence ; right, wide-angle). Reflection from autochthonous Moho marked by arrows. Comparison with the wide-angle data shows that model (a) – 250 m thick lamellae – can be excluded. Model (b) – 100 m thick lamellae – is acceptable. Models (c) and (d) – 500 m thick lamellae, but with a velocity gradient –, although fitting the wide-angle data, produce a high-amplitude Moho reflection at normal incidence that is not observed on the vertical reflection data [after Thouvenot *et al.*, 1990].

FIG. III-9. – *Quatre modèles de vitesse pour le Moho autochtone dans les zones externes (fig. III-2a, traces les plus occidentales) et sismogrammes synthétiques correspondants (à gauche : incidence normale ; à droite, grand angle). Les réflexions émises par le Moho sont soulignées par des flèches. Une comparaison avec les données grand-angle montre que le modèle* (a) *– couches de 250 m d'épaisseur – peut être éliminé. Le modèle* (b) *– couches de 100 m d'épaisseur – est acceptable. Les modèles* (c) *et* (d) *– couches de 500 m d'épaisseur, mais avec un gradient de vitesse –, bien qu'en accord avec les données grand-angle, produit une réflexion à forte amplitude au niveau du Moho en incidence normale, qui n'est pas observée sur les données de la sismique réflexion verticale [d'après Thouvenot* et al., *1990].*

quencies can be observed for the northern fan. This particularity is clearly not to be related to any source effect, since we use here the same shot. It points evidently to a change in the structure than can be caused by three phenomena : (i) a lateral change in the quality factor, i.e. loss of high frequency by anelastic attenuation in the thickened crust, (ii) an introduction towards the east of lamellation in the middle crust, thin layers of alternating high and low velocity, that screen high frequencies from further penetration and may for example contribute to the enhancement of S-wave reflectivity as shown in figure III-7, (iii) a change of the Moho discontinuity to a complex transitional boundary reflecting only long wavelengths. These differents facets will form the object of the next section.

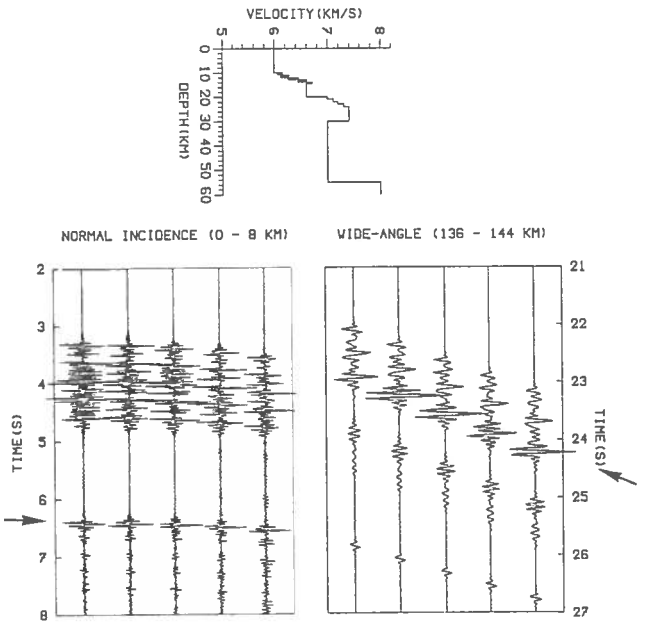

FIG. III-10. – An example of deep-crustal velocity model for the inner zone (fig. III-3a, easternmost traces) and corresponding synthetic seismograms (left; normal incidence; right, wide-angle). Reflection from allochthonous Moho marked by arrows [after Thouvenot *et al.*, 1990].

FIG. III-10. – *Exemple de modèle de vitesse pour les zones internes (fig. III-3a, traces les plus orientales) et sismogramme synthétique correspondant (à gauche : incidence normale ; à droite : grand angle). Les réflexions du Moho allochtone sont marquées par des flèches [d'après Thouvenot* et al., *1990].*

III.G. – SYNTHETIC SEISMOGRAMS FOR DEEP-CRUSTAL LAYERINGS

Figure III-2a reveals a clear change in the Moho reflectivity : to go from one extreme to another, the wavelet reflected for the Moho in the external zone (westernmost traces) can be clearly identified, whereas the reflectivity of the shallow reflector in the inner zone (easternmost traces) is very dull. In the first place, vertical seismics show a reflective lower crust [Bayer *et al.*, 1987; Mugnier *et al.*, 1990], that is almost transparent to wide-angle seismics. In the other place, as shown above, a very reflective zone can be seen on the VRL beneath Vanoise and Gran Paradiso (fig. III-5a).

To investigate these variations, we used the discrete wavenumber method [Bouchon, 1981] to compute synthetic seismograms for different velocity models in the external and inner zones (figs. III-9 and 10). The crust was assumed to be flat-layered, excluding any lateral heterogeneities. For simplicity and because we are here interested in deep reflections, the upper crust was modelled as a single layer with a constant 6 km.s^{-1} velocity. Introducing any further layering in this part of the model would only alter the early part of the seismograms, which is beyond the scope of this study. The computation of the direct wave was also suppressed for the same reason. Wherever lamellae were introduced in the models, their thicknesses and velocities were randomized in order to avoid any misleading constructive interference effect.

For each model, two sets of synthetic traces are presented : (i) normal incidence, with 5 receivers in the 0-8 km distance range; (ii) wide-angle incidence, with 5 receivers around 90 km (external zone) or 140 km (inner zone). To account for the difference in the spectral response of the geophones used in the wide-angle experiment and vertical seismics, we used 2 source signals with different frequency bands : 9-22 Hz for normal incidence, 4-11 Hz for wide-angle.

Figure III-9 addresses the autochthonous Moho in the external zone (refer to the wide-angle data, fig. III-2a, westernmost traces). Example (a) shows a lower crust modelled as a heap of lamellae with an average thickness of 250 m and velocities alternating between low values (about 6 km.s^{-1}) and high values (about 7 km.s^{-1}). Even if it provides a satisfactory normal incidence section with a seismic layering between 10 and 12 sec, it is not acceptable because the synthetic wide-angle section shows high amplitude arrivals reflected from the lamellae that mask much of the Moho reflection. Decreasing slightly the average thickness of the lamellae to 100 m (fig. III-9b) makes the lower crust transparent to low-frequency wide-angle incident waves, and the Moho reflection comes out more clearly. The normal incidence section shows a reflection pattern that is not as even as in figure III-9a, with a high reflectivity in the top of the lower crust and a more transparent band with the Moho reflection at its bottom. This pattern is very similar to what is observed on the VRL data in the external zone, as described for instance by Bayer *et al.* [1987].

If we do not stick to this oversimplified model of the lower crust and introduce a velocity gradient in the layering, figure III-9c and d show that the average thickness of the lamellae, here taken as 500 m, is not as critical as in examples (a) and (b) : thanks to weaker velocity contrasts in the top part of the lower crust, less energy is reflected at wide-angle and the Moho reflection remains prominent. The synthetic wide-angle sections are thus not that much different from the one obtained for model (b). However, the synthetic normal incidence sections in (c) and (d) show an increase in the reflectivity with depth, with the Moho reflection being the highest amplitude arrival. As we do not recognize this feature on the VRL data, we eventually prefer model (b), even if it is rather clear that many intermediate models would also be acceptable.

The case of the allochthonous Moho in the inner zone (refer to the wide-angle data, fig. III-2a, easternmost traces) is only skimmed over in figure III-10. It shows that a transitional shallow Moho, modelled as a gradient zone overlain by a few 500-m thick layers gives a dull reflection within a rather long wavetrain in the wide-angle synthetic section. Its normal incidence image is on the contrary quite clear, with distinct arrivals of reflected energy. It should be stressed however that we have no actual control on the velocity distribution neither within the shallow reflective unit nor underneath.

III.H. – TECTONIC IMPLICATIONS AND CONCLUSIONS

The first result of the wide-angle experiment was to demonstrate the Moho existence from the foreland to the root zone. Even if the Moho reflectivity is variable, its topography is now well documented and this geometry is now to be taken into account in any structural reconstruction of the Alpine belt. No vertical disappearence of the Alpine "roots" can be observed.

In the external zone, we investigated different lower-crustal layerings by the computation of synthetic seismograms. A qualitative comparison with the VRL and wide-angle data shows that using both data sets brings more

constraints, as already shown by Braile and Chiang [1986]. Our preferred model for the autochthonous Alpine lower crust is a heap of 100-m thick lamellae with velocities alternating between 6 $km.s^{-1}$ and 7 $km.s^{-1}$.

The relative shallow reflector discovered beneath the Briançonnais zone was never mapped before, although recent models of Alpine orogeny involving a lithospheric flaking [Ménard and Thouvenot, 1984] already suggested such a feature. In a more external position, we also saw that S-waves from shot-A mapped a reflector in the 25-30 km depth range, but its relation with the Briançonnais reflector is dubious. The seismic signature of the wavelet reflected from the Briançonnais reflector indicates lower-crustal or upper-mantle material and, because the seismic signal is stretched and sustained, one could suspect this reflector to be actually a transition zone rather than a first-order discontinuity. When referring to VRL data, this reflector is shown to underlie a highly-reflective layer. In this aspect, it has a Moho-like behaviour. In stable areas where a layered lower crust is observed, it is now well-established that the Moho corresponds to the lower limit of the layering [Mooney and Brocher, 1987; Holbrook, 1988]. However, it should be stressed that the present data does not give us any control on the actual velocity distribution neither within the reflective unit nor underneath.

The connection of this unit to the Ivrea body, locally reached in our experiment under the Sesia massif, is unlikely because of the depth difference of nearly 20 km between the two reflectors. Linking it to the Po Plain Moho – which would make the Ivrea body a detached mantle unit – would be more plausible. This idea should however be dropped if we consider the very different character of the wavelet reflected from the two reflectors – dull for the Briançonnais Moho and sharp for the hinterland Moho.

Thus, the Moho picture of the western Alps gained both in sharpness and complexity since four segments at least now have to be considered : deep autochthonous Moho, Briançonnais Moho, Ivrea body and Po plain Moho. This makes the reconstruction puzzle more constrained but also more complicated.

As a whole, the fan layout of the experiment proved successful in detecting very deep reflections. The VRL, equipped with 10 Hz geophones [Damotte *et al.*, 1990], was able to provide information on upper and mid-crustal reflectors, but had difficulties in finding out the deep Alpine Moho east of the ECMs. Uniting vertical reflection profiling with the more versatile wide-angle reflection method therefore provides the sort of complementary information required to determine the deep structure of such complex orogens as the Alpine belt.